

Introduction

An all-sky imager (ASI) has been operating at El Leoncito, Argentina (31.8 S, 69.3W, 19.6 S mag lat) since 1999. Plasma depletions associated with equatorial spread F (ESF) have been consistently observed at this location with a 630 nm filter. In October 2014 an ASI was installed at Villa de Leyva, Colombia (5.6 N, 73.52 W, 16.3 N mag lat) such that its field of view includes the magnetic conjugate point of the El Leoncito ASI. Figure 1 shows images from these two sites and from Jicamarca (-11.95 S, 76.87 W, -0.1 S mag lat), installed in March 2014. The images show a 160° field of view unwarped at an altitude of 250 km. This configuration will allow us to concurrently observe airglow structures associated with bottomside and topside ESF. The sites at Colombia and Argentina are conjugate to each other allowing us to investigate how depletions behave at the foot points of common flux tubes.

Objectives and Goals:

In this study we use observations from three ASIs in South America during times of visible plasma depletions associated with ESF to study background conditions affecting the properties of airglow depletions.

We investigate how ESF depletions vary between the two conjugate sites. There are two characteristics that we look at:

- 1) We compare the velocity of the depletions
- 2) We compare the background emission and contrast between the background and the depletion

We also use the ASI at Jicamarca to investigate wave structuring of airglow depletions. We measure the separation of bottomside ESF structures to look for evidence of large scale wave structures.

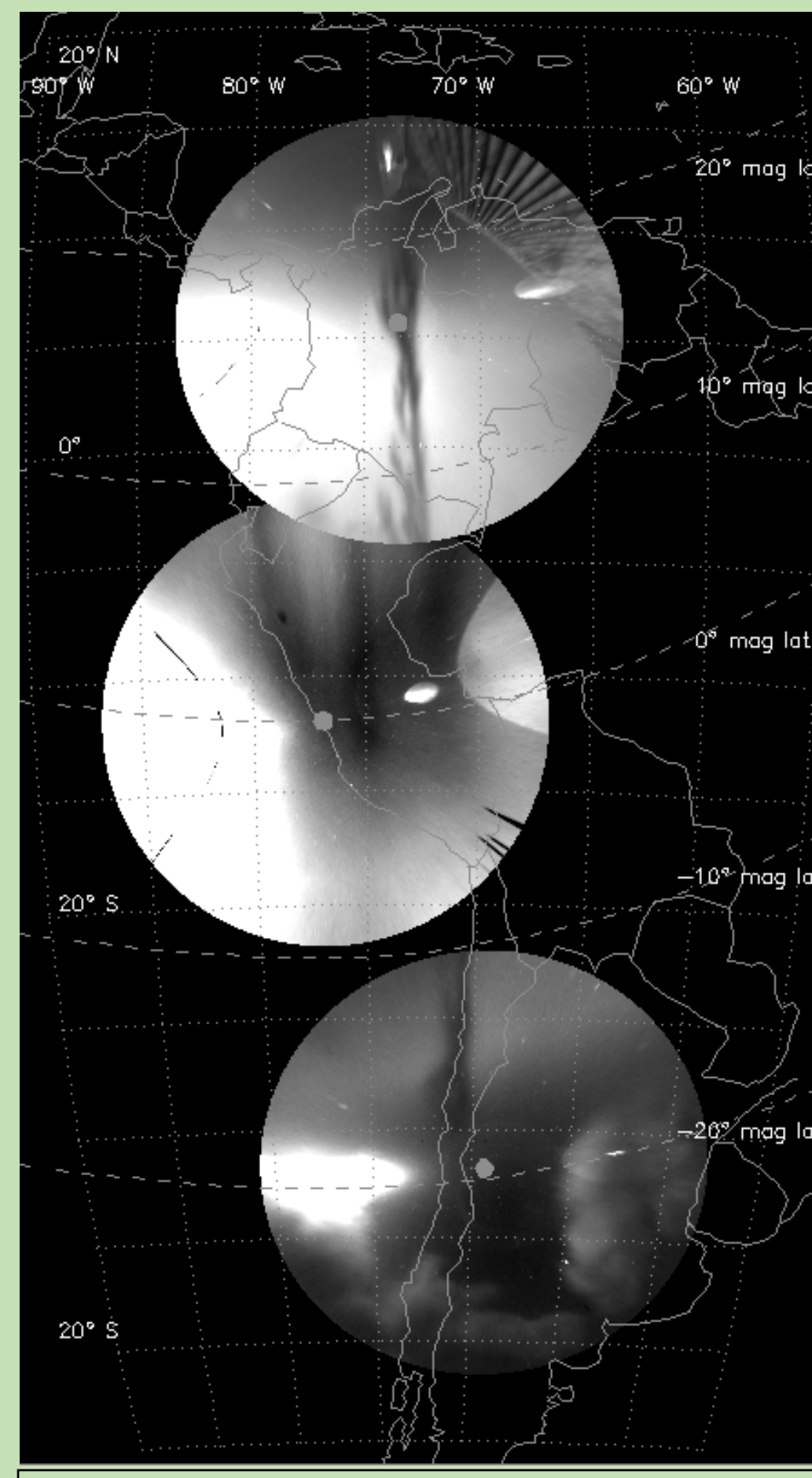


Figure 1: A map showing unwarped images at three sites in South America from 2:45 UT on 20 Oct 2015

1.) Depletion Velocities at Conjugate Sites

We compare the zonal velocity of depletions at Villa de Leyva and El Leoncito around the equinoxes and December solstice. Around June solstice we do not have enough data at both sites to determine velocities. Figure 2 shows images taken from 10 March 2015. The asterisk indicates the latitude where the velocities are measured. We track the position of the depletion for as long as it is visible to determine the velocity.

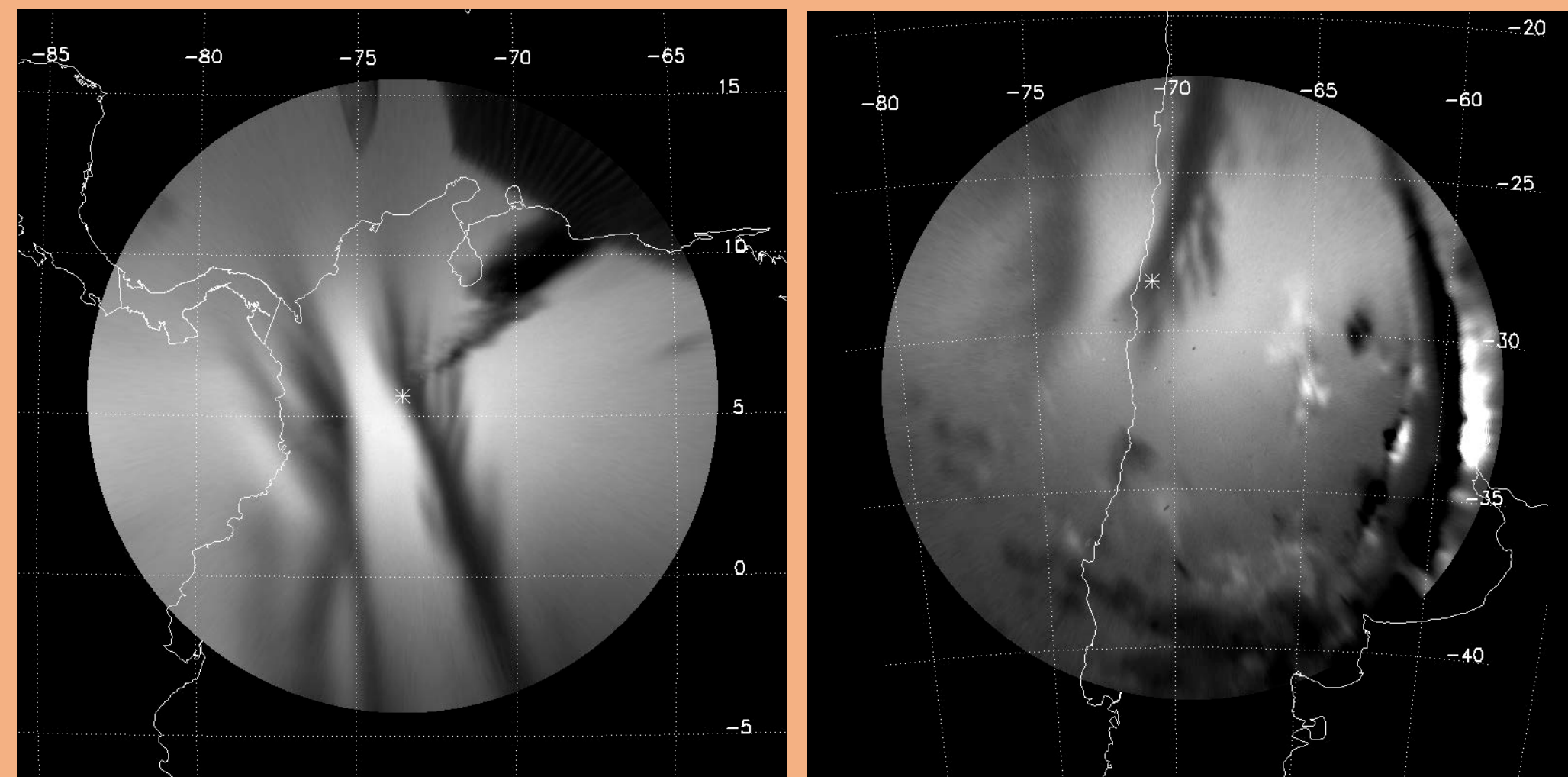


Figure 2: Unwarped ASI images at Villa de Leyva (left) and El Leoncito (right) at about 2UT on 10 March 2015. The asterisk indicates the location of the conjugate points where the cuts were taken.

Figure 3 shows the resulting zonal velocities averaged over multiple depletions from three different nights. For all three cases presented here we see that El Leoncito has a greater velocity for most of the night.

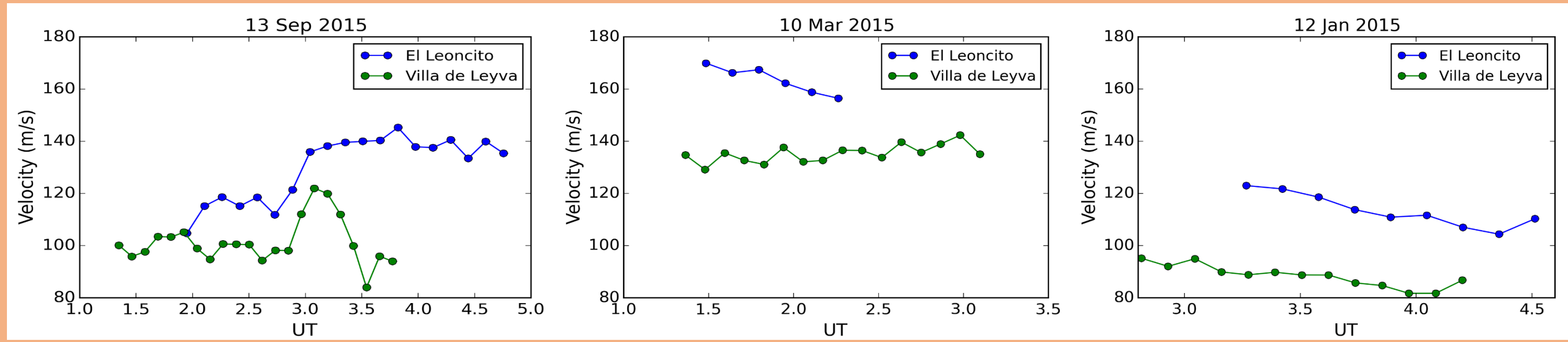


Figure 3: Zonal velocities from 13 Sep 2015, 12 Jan 2015, and 10 Mar 2015. The uncertainty in the determination is around 30%.

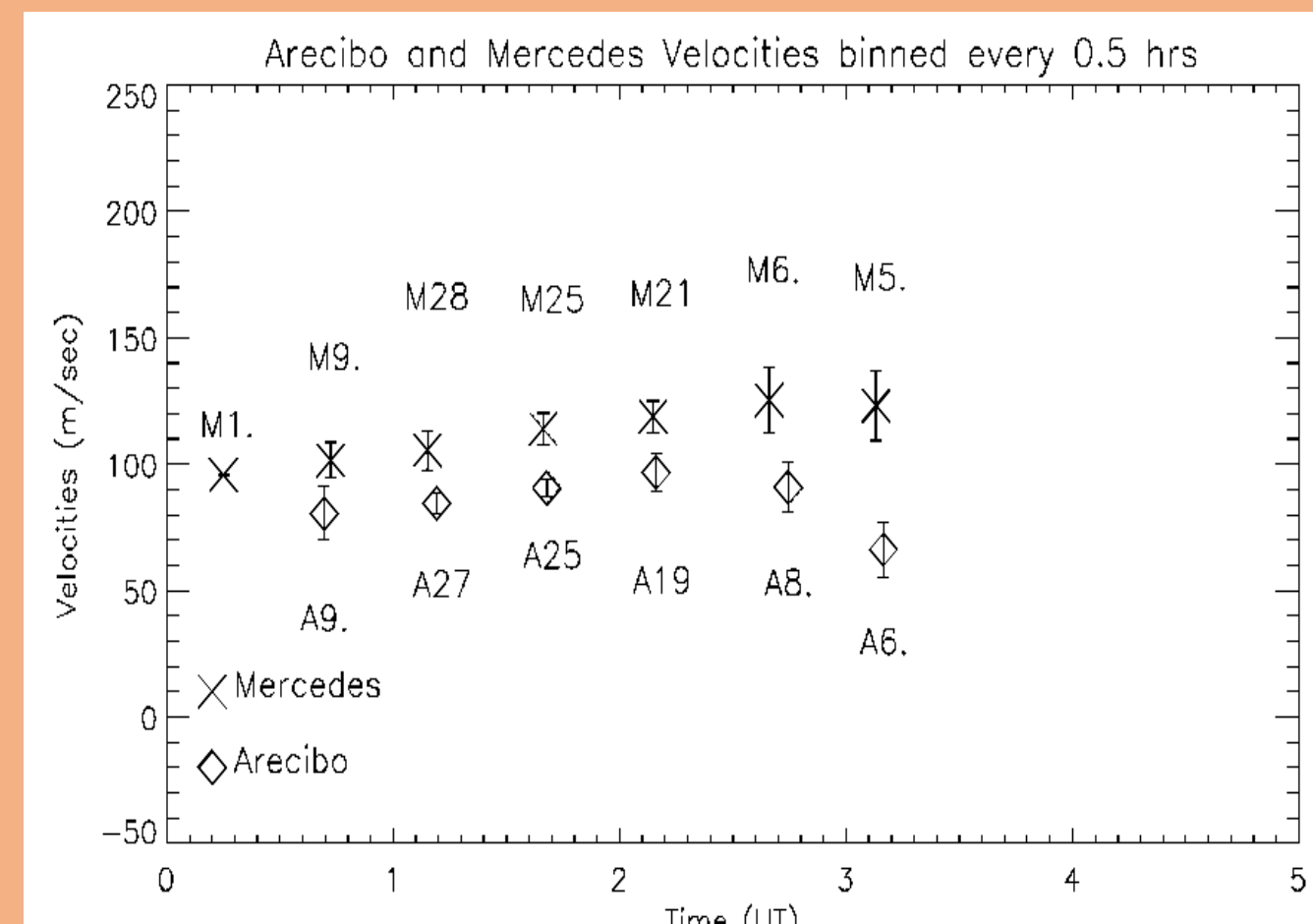


Figure 4: Averaged velocities from Arecibo and Mercedes.

Figure 4 shows average results from another set of conjugate imagers at Arecibo in Puerto Rico and Mercedes in Argentina, approximately 10° to the east of El Leoncito (Martinis et al., in prep). Data were taken during equinox conditions from 2010-2012. The numbers following each letter indicate the number of data points used to obtain the average result. This is consistent with our results from Villa de Leyva and El Leoncito that the zonal velocities are greater at the southern end of the magnetic field line. Calculations of plasma drifts based on a realistic geomagnetic field show that in the southern hemisphere one can expect a 30% increase in the zonal velocities, a direct consequence of weaker magnetic fields. We use a tool to

compute conjugate zonal velocities developed by V. Eccles at Space Environment Corporation. It involves IGRF field-line tracing and assumes an electrostatic approximation. The model is consistent with the comparisons between the two conjugate sets, with stronger differences in velocity to the east.

2.) Seasonal Influence on Background Brightness and ESF Contrast

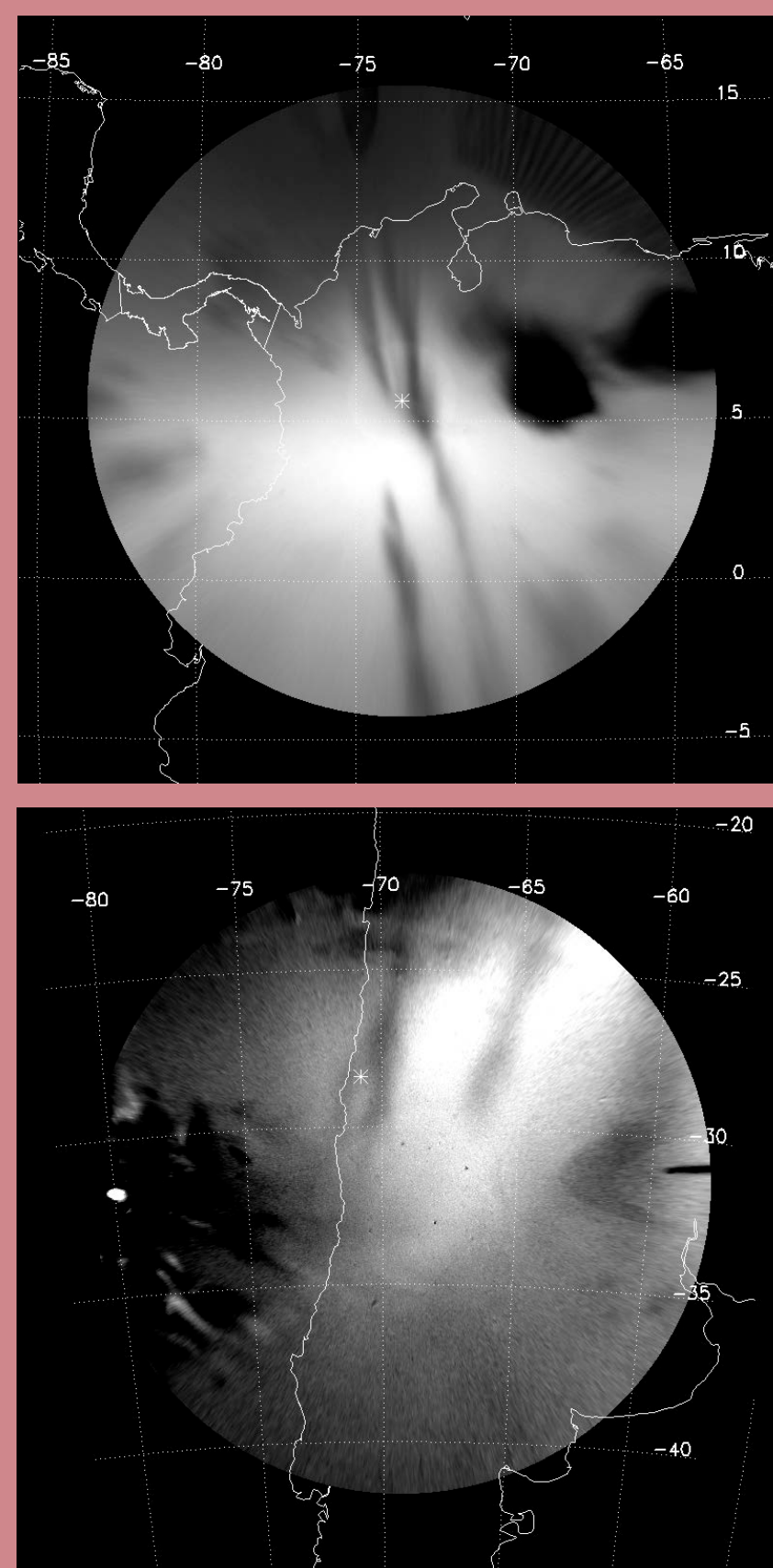


Figure 5: Unwarped ASI images at El Leoncito (bottom) and Villa de Leyva (top) at about 4UT on 29 November 2014. The asterisk indicates the location of the conjugate points where the cuts were taken.

Villa de Leyva has plasma at lower altitudes which increases 630 nm emission since it is dependent on electron and neutral densities. We compare the integrated emission rate from the model with the calibrated images in Table 1 and find that it successfully predicts lower emission for El Leoncito but does not accurately predict the absolute intensity at Villa de Leyva. Table 1 also compares the depletion emission and ratio with the background and we find them to be different.

There is often a difference in the background emission and in the contrast between the depletion and the background at conjugate sites. In Figure 2 the brightness in the images appears similar because they have been adjusted for visibility. Figure 5 shows another case from 29 November 2014 where the difference between the images is more apparent. Figure 6 shows absolute intensity at latitudes marked by the asterisks in Figures 2 (left) and 5 (right).

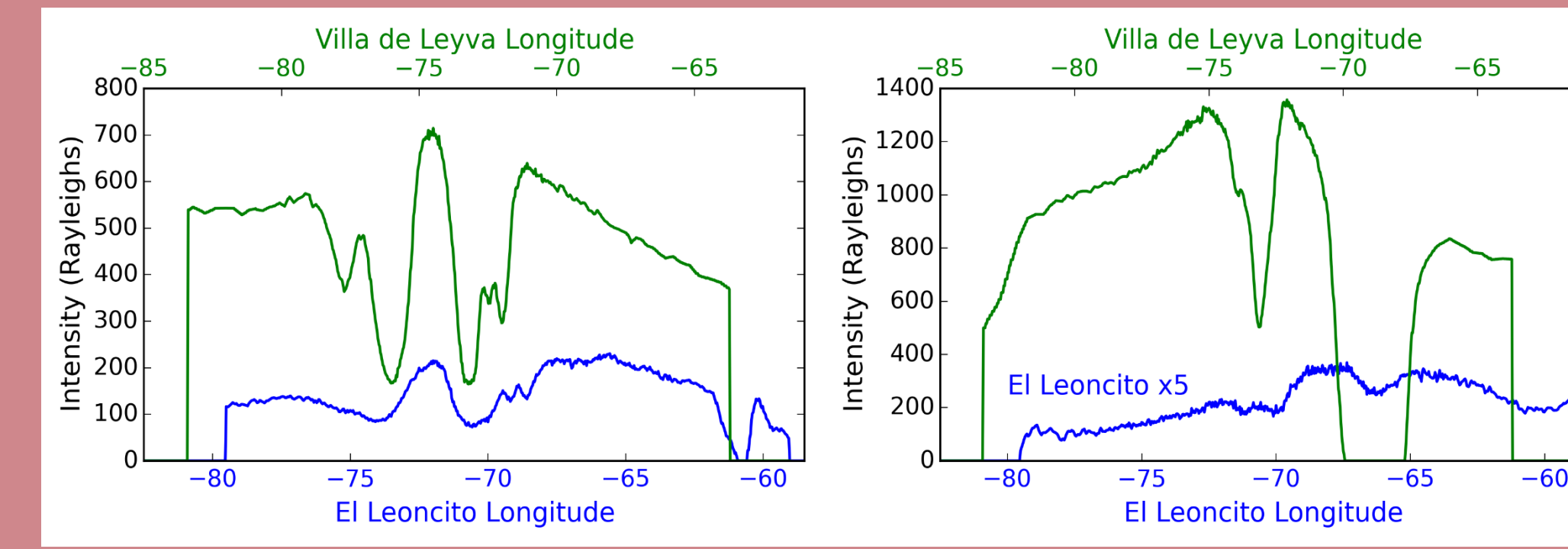


Figure 6: Cuts through Figure 2 (left) and Figure 5 (right) at the points marked in the images showing the absolute intensity

On both nights Villa de Leyva has higher emission than El Leoncito, but the difference is greater in November. We use the BU airglow model to determine the emission. Inputs for the model are taken from IRI-2012 (Bilitza, 2015) and NRLMSISE-00 (Picone et al., 2002). Modeled emission are shown in Figure 7. Figure 8 shows the electron density profiles for the two sites to determine why El Leoncito has a lower emission rate during both nights.

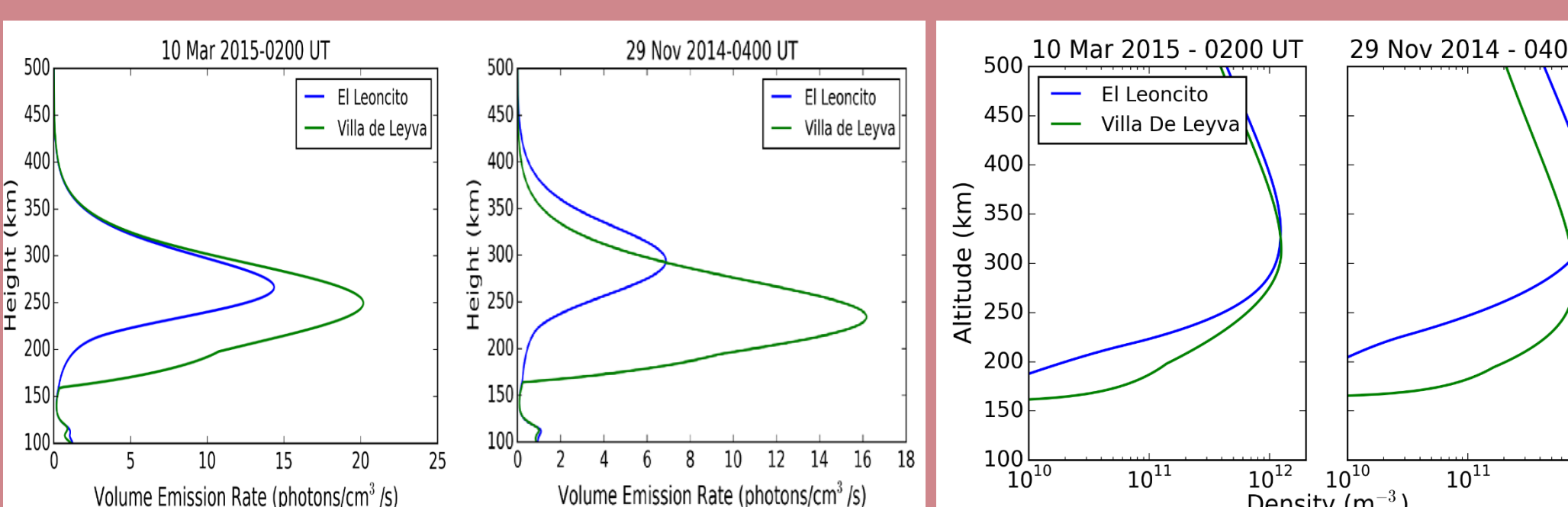


Figure 7: Modeled 630.0 nm emission at the two conjugate locations.

Figure 8: Models of electron density for the two cases shown

	El Leoncito				Villa de Leyva			
	Background Data	Depletion Model	Ratio Data		Background Data	Depletion Model	Ratio Data	
Mar	210 R	131 R	80 R	0.38	700 R	230 R	168 R	0.24
Nov	70 R	72 R	35 R	0.5	1320 R	170 R	502 R	0.38

Table 1: Comparison between measured and modeled background emission and the ratio between the depletion and the background.

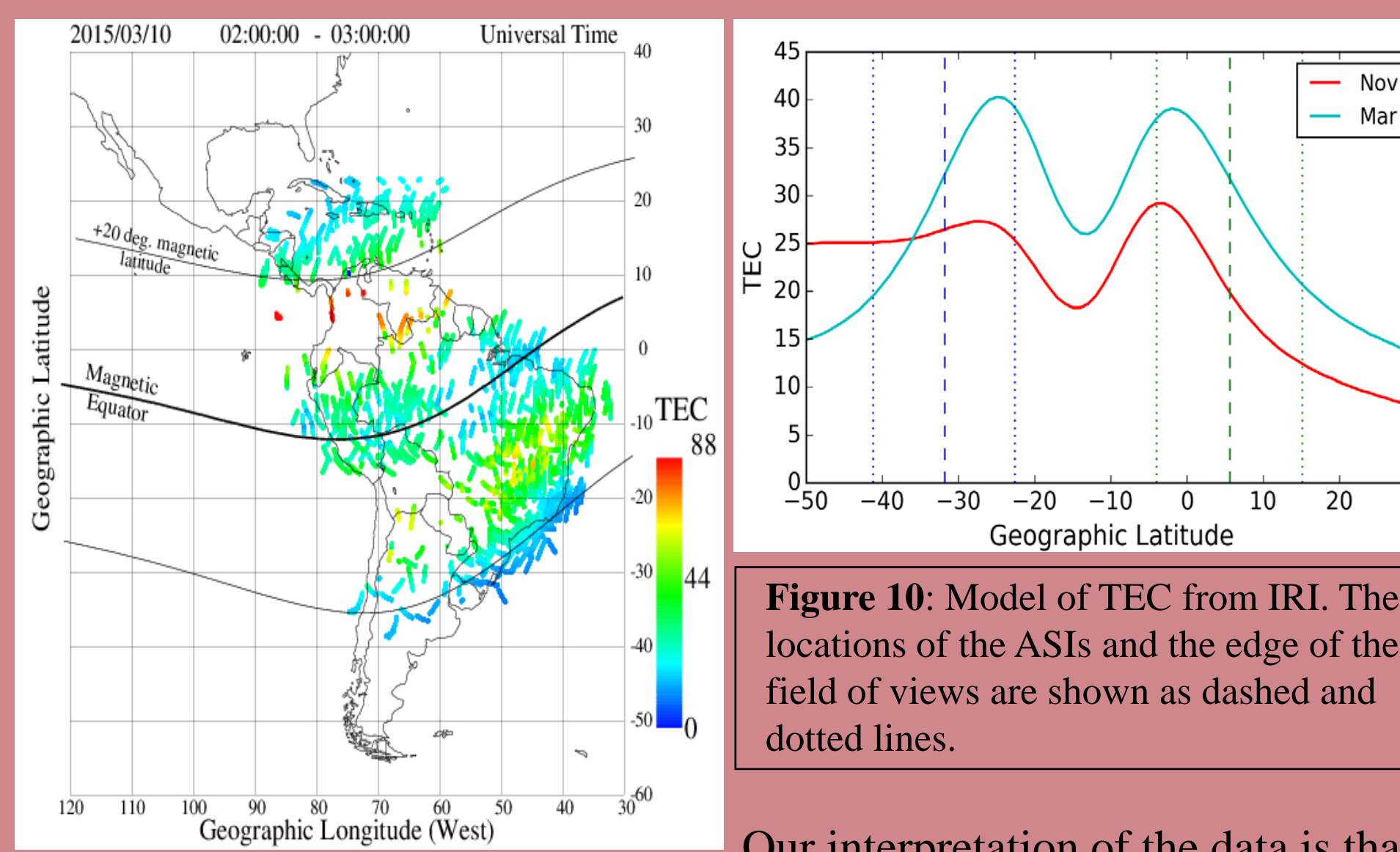


Figure 9: Measured TEC on 10 March 2015 from GPS in the Low latitude Ionosphere Sensor Network (LISN).

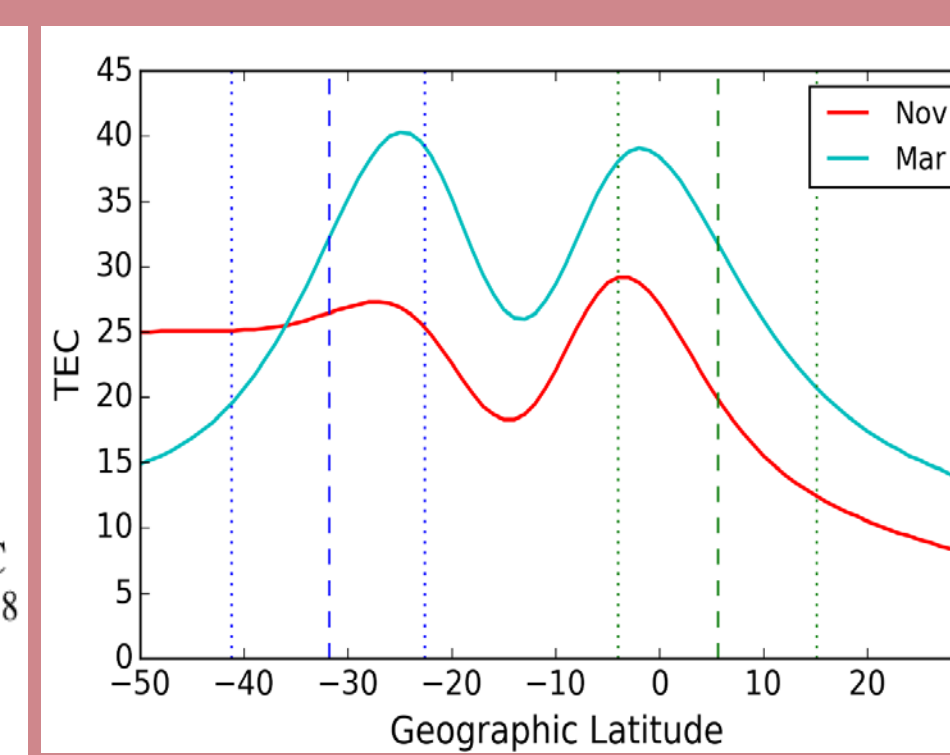


Figure 10: Model of TEC from IRI. The locations of the ASIs and the edge of their field of views are shown as dashed and dotted lines.

Our interpretation of the data is that meridional winds play a large role as well. As seen in Figure 11, around December solstice meridional winds at both locations are mostly northward which can move plasma up and away from El Leoncito and increase the plasma density at Villa de Leyva. Around equinoxes winds are slower and at both sites they are equatorward, giving similar emission at each site. In these cases the crest of the anomaly is right over Villa de Leyva but this is not predicted by IRI. This seems to be the major source of discrepancy between our results and the model results.

We use measured TEC to compare with the model. Figure 9 shows a map of TEC for the March case. Figure 10 shows modeled TEC versus latitude. Table 2 summarizes the differences between the modeled and measured TEC.

	El Leoncito		Villa de Leyva	
	Data	Model	Data	Model
Mar	40	32	80	32
Nov	10	19	70	12

Table 2: Comparison between measured and modeled TEC

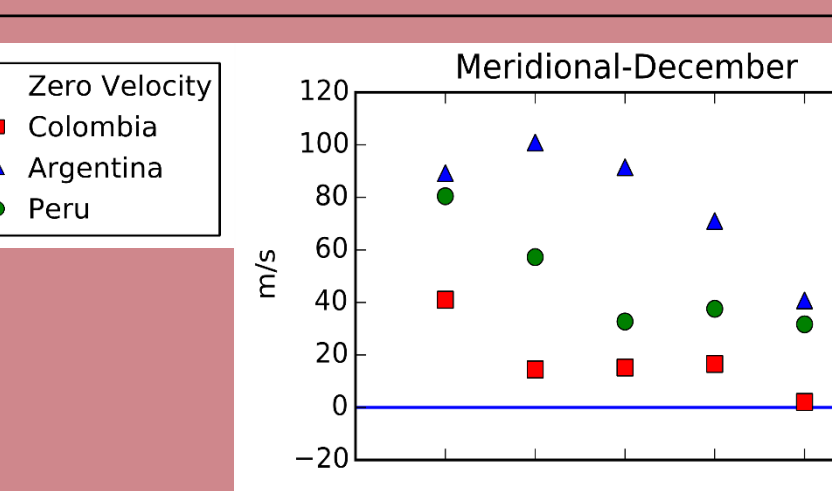


Figure 11: Seasonal meridional winds at Jicamarca, El Leoncito and Villa de Leyva from HWM14

3.) ESF Modulation by Large Scale Waves

The third ASI that we routinely use is located at the magnetic equator at Jicamarca. This imager is used to measure this distance between plasma depletions in order to see if there is modulation of the structures by waves. A previous study by Tsunoda and White (1981) showed that a 400 km large scale wave structure modulated the production of ESF (Figure 13).

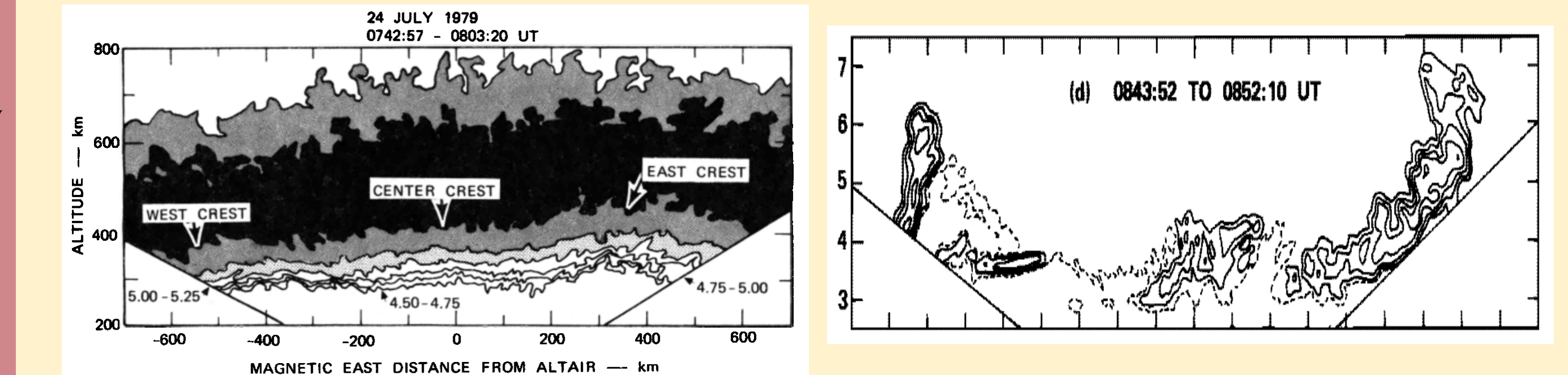


Figure 13: Large scale wave structure and subsequent ESF from Tsunoda and White (1981)

Additionally, the distance between plasma depletions associated with ESF has been measured during solar minimum using imagers in Chile (Makela et al., 2010), Christmas Island, and Brazil (Chapagain et al., 2011). They both measured the spacing between adjacent plasma depletions and found that the structures were typically separated by 100-300 km. The observations from Makela et al. (2010) were interpreted as being the result of gravity waves.

We looked at 517 nights of data, from 2014-2015 during solar maximum, and in 120 of them we were able to observe bottomside ESF. Almost every clear night showed depletions. We measured the smaller distance between the depletions within the groups and measured the distance between the groups. Observations showed multiple depleted structures in close groups of 2-4 that were separated from other groups by a larger distance. Examples of this grouping are shown in Figure 14.

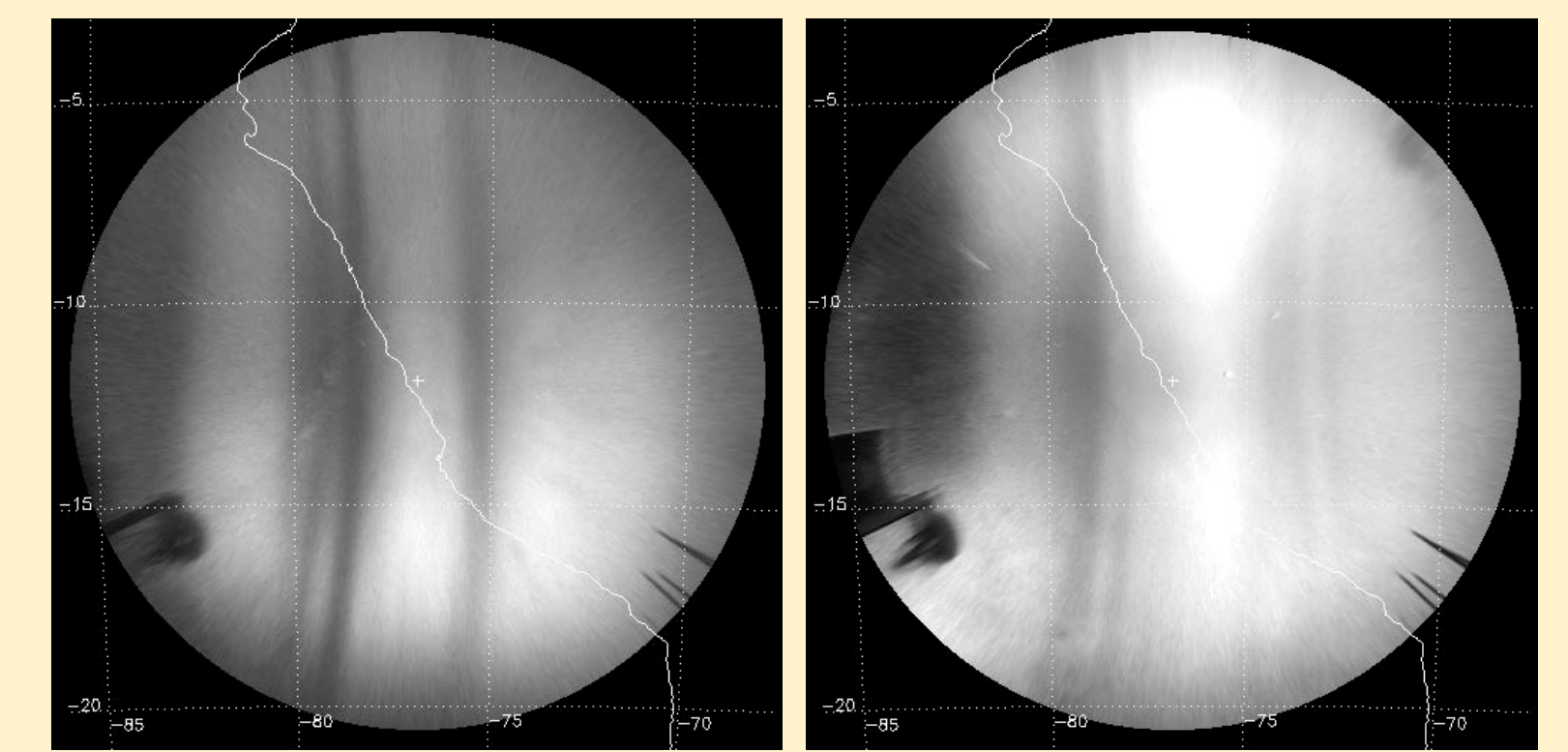


Figure 14: Example of depletion grouping from 19 Aug, 2015 (left) and 3 April, 2014 (right)

We found that the typical distance within the groups was about 100 km and the group to group separation was 400-500 km

Almost every night shows depletions with this type of grouping. Our separation distances at solar maximum are not significantly different from solar minimum results and we found no seasonal dependence on the grouping or separation.

Summary

- We compared the velocities of depletions at conjugate sites and found that velocities at El Leoncito in the Southern Hemisphere tended to be greater than those at Villa de Leyva in the Northern Hemisphere. This is a result of the weaker magnetic field in the Southern Hemisphere.
- Large variations in background emission and ESF contrast between conjugate sites are observed. These are largely impacted by the location of the equatorial anomaly crests as well as seasonal differences in meridional winds.
- ESF depletions observed at Jicamarca tend to come in groups of 2-4 separated by about 450 km on average confirming the recurrent presence of waves of this scale in ESF characteristics. Within the group the separation is about 100 km.

Acknowledgements

We thank the directors and personnel of the El Leoncito, Villa de Leyva, and Jicamarca observatories. This work was supported by NSF Aeronomy Grants #1153264 and # 0724440. TEC data was taken from the LISN website (<http://lisn.igp.gob.pe/data/>). LISN is a project led by Boston College in collaboration with the Geophysical Institute of Peru and other institutions that provide information in benefit of the scientific community.

References

Bilitza, D. (2015). The international reference ionosphere - Status 2013. *Adv. Sp. Res.*, 55(8), 1914-1927. doi:10.1016/j.asr.2014.07.032.
 Picone, J. M., A. E. Hedin, D. P. Drob, and A. C. Aikin (2002). NRLMSISE-00 empirical model of the atmosphere: Statistical comparisons and scientific issues. *J. Geophys. Res. Sp. Phys.*, 107(A12), SIA 15-1-SIA 15-16. doi:10.1029/2002JA009430.
 Chapagain, N. P., M. J. Taylor, and J. V. Eccles (2011). Airglow observations and modeling of F region depletion zonal velocities over Christmas Island. *J. Geophys. Res. Sp. Phys.*, 116(C2), doi:10.1029/2010JA015958.
 Makela, J. J., S. L. Vadas, R. Muryanto, T. Duly, and G. Crowley (2010). Periodic spacing between consecutive equatorial plasma bubbles. *Geophys. Res. Lett.*, 37(14), 1-5. doi:10.1029/2010GL043968.
 Mendillo, M., E. Zesta, S. Shobhan, P. J. Sultan, R. Doe, Y. Sahai, and J. Baumgardner (2005). Observations and modeling of the coupled latitude-altitude patterns of equatorial plasma depletions. *J. Geophys. Res. Sp. Phys.*, 110(A9), 1-7. doi:10.1029/2005JA011157.
 Tsunoda, R. T., and B. R. White (1981). On the generation and growth of equatorial backscatter plumes 1. Wave structure in the bottomside F layer. *J. Geophys. Res.*, 86(A5), 3610. doi:10.1029/JA086iA05p03610.